Limits of NbTi and Nb_3Sn, and Development of W&R Bi–2212 High Field Accelerator Magnets

A. Godeke, D. Cheng, D. R. Dietderich, P. Ferracin, S. O. Prestemon, G. Sabbi, and R. M. Scanlan

***Abstract*— NbTi accelerator dipoles are limited to magnetic fields (H) of about 10 T, due to an intrinsic upper critical field (H_{c2}) limitation of 14 T. To surpass this restriction, prototype Nb_3Sn magnets are being developed which have reached 16 T. We show that Nb_3Sn dipole technology is practically limited to 17 to 18 T due to insufficient high field pinning, and intrinsically to 20 to 22 T due to H_{c2} limitations. Therefore, to obtain magnetic fields approaching 20 T and higher, a material is required with a higher H_{c2} and sufficient high field pinning capacity. A realistic candidate for this purpose is Bi–2212, which is available in round wires and sufficient lengths for the fabrication of coils based on Rutherford-type cables. We initiated a program to develop the required technology to construct accelerator magnets from 'wind-and-react' (W&R) Bi–2212 coils. We outline the complications that arise through the use of Bi–2212, describe the development paths to address these issues, and conclude with the design of W&R Bi–2212 sub-scale magnets.**

***Index Terms*— Accelerator magnet, HTS, Bi–2212**

I. Introduction

THE superconducting material of choice for accelerator magnets has long been NbTi. The world's largest particle accelerator, the Large Hadron Collider (LHC) at CERN, utilizes NbTi technology. The record magnetic field with NbTi in a dipole configuration is 10.5 T at 1.8 K [1], and is approaching the intrinsic limitations of NbTi as will be discussed below. To surpass the intrinsic limitations of NbTi, a number of prototype dipole magnets have been constructed using Nb_3Sn superconductors, since Nb_3Sn approximately doubles the available field–temperature regime. Prototype dipole magnets that utilize Nb_3Sn technology reach a steadily increasing magnetic field, with the present record being 16 T at 4.5 K [2]. This progress resulted, for a significant part, from the increasing critical current density (J_c) in strands [3].

These successful prototype magnets demonstrate the feasibility of Nb_3Sn for use in accelerator magnets. This is emphasized through the U.S. LHC Accelerator Research Program (LARP) [4], which focuses on the development of Nb_3Sn magnets for future LHC upgrades. However, as will be shown below, due to these recent successful efforts, Nb_3Sn magnets are also rapidly approaching the material's limitations and a switch to a new material is inevitable to achieve higher magnetic fields.

Manuscript received September 1, 2006. This work was supported by the Director, Office of Science, High Energy Physics, U.S. Department of Energy under contract No. DE-AC02-05CH11231.

A. Godeke (corresponding author; phone: +1-510-486-4356; e-mail: agodeke@lbl.gov), D. Cheng, D. R. Dietderich, P. Ferracin, S. O. Prestemon, G. Sabbi, and R. M. Scanlan are with Lawrence Berkeley National Laboratory, One Cyclotron Rd, Berkeley CA 94720.

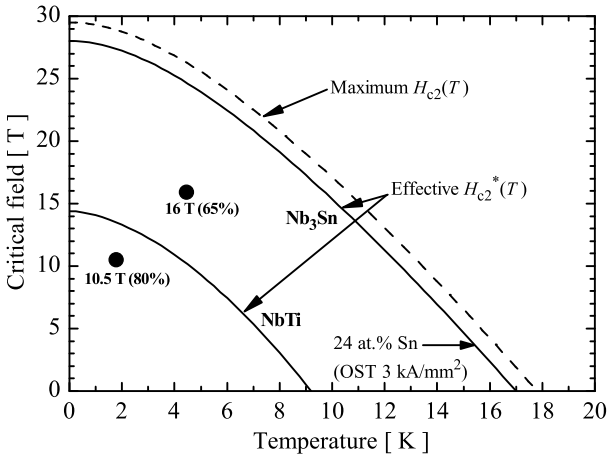

Fig. 1. Field-temperature phase boundaries and record magnetic fields in dipole magnets for NbTi and Nb_3Sn.

II. Magnetic field limits using NbTi and Nb_3Sn

To validate the use of a new material and the ensuing technology development, an accurate determination of the limitations of the present materials is required. A material's current carrying capacity is determined by its effective field-temperature phase boundary ($H_{c2}^*(T)$) and its pinning capacity. A material's pinning force (F_p) is maximized when the pinning site density is comparable to the flux-line density in the operating magnetic field range.

For NbTi, $H_{c2}^*(T)$ is limited by $H_{c2}^*(0) \cong 14.4$ T and an effective critical temperature $T_c^*(0) \cong 9.2$ K [5], as depicted in Fig. 1. Pinning sites can be engineered in NbTi in the form of α–Ti precipitates, with a spacing that is comparable to the flux-line spacing in the 5 to 10 T magnetic field range [6] (Fig. 2). NbTi is therefore, under present understanding, close to fully optimized. This pinning capacity optimization yields a parabolic-like $F_p(H)$ that peaks at about 50% of H_{c2}^* [5], and a maximum $J_c(5\ \mathrm{T}, 4.2\ \mathrm{K}) \cong 3$ kA/mm^2, or 1150 A/mm^2 at 8 T and 4.2 K [1]. Fig. 1 shows that an optimized dipole magnet, using an optimized NbTi wire, achieves about 80% of its intrinsic field-temperature limitation. 80% can thus be regarded as an optimized efficiency for dipole magnets.

Recent investigations on the capacities of Nb_3Sn superconductors [7]–[9] place well-defined practical and intrinsic limitations on its performance. For Nb_3Sn, being stable from about 18 to 25 at.%Sn (the A15 phase), $H_{c2}^*(T)$ depends on the H_{c2} averaging over the compositions that are present in a wire [9]. In Fig. 1, the maximum detectable $H_{c2}(T)$ in

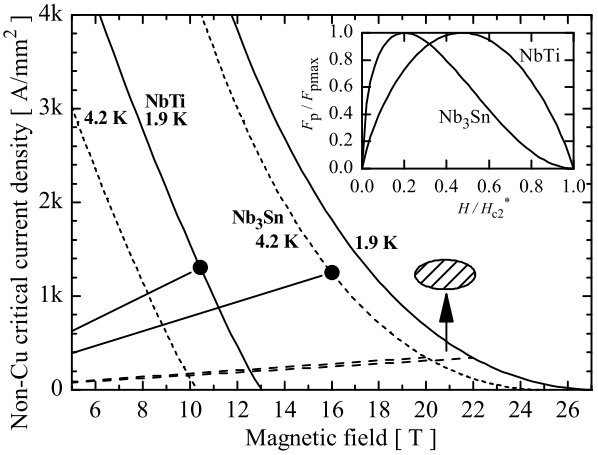

Fig. 2. Critical current density as function of magnetic field at 1.9 and 4.2 K in NbTi and Nb_3Sn. Included are the load-lines for record magnets and for a hypothetical Nb_3Sn dipole magnet achieving 80% of its intrinsic limitation. The inset shows the normalized pinning force as function of reduced magnetic field.

wires is depicted by the dashed line. Also a best estimate is given for $H^*_{c2}(T)$ for the present record Internal Tin (IT) wire ($J_c(12\ \mathrm{T},\ 4.2\ \mathrm{K}) = 3$ kA/mm^2) [3], which has an average Sn content of 24 at.%Sn [10]. This $H^*_{c2}(T)$ is limited by $H^*_{c2}(0) \cong 28$ T and $T^*_c(0) \cong 17$ K. Fig. 1 shows that the present record dipole magnet, using the present record wire, achieves about 65% of this $H^*_{c2}(T)$. If Nb_3Sn, like NbTi, would achieve 80% of $H^*_{c2}(T)$, it would reach a dipole magnetic field of 20 T at 4.2 K, or 22 T at 1.9 K, which forms an intrinsic magnetic field limitation for Nb_3Sn, which is closely approached in graded solenoids.

The main reasons why a Nb_3Sn accelerator magnet does not achieve 80% of its intrinsic limitation is lack of high field pinning capacity, combined with the use of ungraded systems. Grain boundaries are the main pinning centers in Nb_3Sn and the average grain size in commercial wires is between 100 to 200 nm [7]. The average flux-line spacing, in contrast, is about 10 to 15 nm. The flux-line density is therefore about one order of magnitude larger than the grain boundary density. This results in collective pinning of the flux-line lattice, described by an asymmetric $F_p(H)$ that peaks at only 20% of H^*_{c2}, i.e. at about 5 T at 4.2 K for the present record IT wires [8] (Fig. 2). This lack of high field pinning translates to the concave $J_c(H)$ curves in Fig. 2, and a reduced current carrying capacity towards H^*_{c2} [8]. The pinning curve for optimized NbTi, in contrast, translates to an approximately linear $J_c(H)$ reduction up to H^*_{c2} [5].

It has been demonstrated that the introduction of additional pinning sites in Nb_3Sn causes the maximum in $F_p(H)$ to increase and shift towards higher magnetic field [11]. Therefore, the only way to retain current carrying capacity in Nb_3Sn when approaching H^*_{c2} (as indicated by the hatched region in Fig. 2) is by an enhancement of the pinning site density through grain refinement or the inclusion of engineered pinning centers. Both these options, though demonstrated on laboratory samples, have not yet been validated in commercial wires. Grading and an unlimited conductor package could, in theory, generate magnetic fields approaching 20 T, but the resulting magnets would be unpractically large and expensive due to Nb_3Sn's in-efficiency at high magnetic fields. Nb_3Sn is therefore exhausted at dipole magnetic fields in the 17 to 18 T region. Even if high field pinning capacity in wires could be improved, Nb_3Sn would still be intrinsically limited to 22 T at 1.9 K as described above.

To progress towards magnetic fields of 20 T and higher, it is thus inevitable to switch to a new material with a significantly higher H_{c2} and sufficient high field pinning capacity. Of the possible candidate materials ($YBa_2Cu_3O_{7-\delta}$, $Bi_2Ca_2CuSr_2O_{8+x}$, $Bi_2Ca_2Cu_2Sr_3O_{10+y}$, MgB_2), only Bi–2212 is sufficiently developed for use in accelerator magnet applications. It has an $H^*_{c2}(4.2\ \mathrm{K})$ of about 85 T [12], a NbTi-like pinning curve, and is available in round wires with sufficient length. The latest generation Bi–2212 wires have already demonstrated to surpass the overall (engineering) critical current density in Nb_3Sn wires at magnetic fields of about 18 T and higher [13].

III. Technological challenges with Bi–2212

Constructing a magnet using Bi–2212 is significantly more complicated than using NbTi or Nb_3Sn, as summarized in Table I. Technological challenges are related to the strain sensitivity of Bi–2212, its high formation reaction temperature in an oxygen-rich environment, and chemical compatibility of the insulation and construction materials during the reaction heat treatment. Operational challenges are related to the low normal zone propagation velocity, hindering energy dissipation and quench detection.

A. Stress and strain related issues

The critical current in Bi–2212 is, like Nb_3Sn, sensitive to strain (ϵ). A model that has been developed to describe the behavior of $J_c(\epsilon)$ in Bi–2212 in longitudinal strain experiments indicates, as with Nb_3Sn, that the highest J_c is obtained in the strain free state (Fig. 3 [14]). Compressive axial strain during cool-down causes, in contrast to Nb_3Sn, an *irreversible* reduction of J_c (Fig. 3: *a*). Releasing the thermal pre-compression (Fig. 3: *b*) does not, as for Nb_3Sn, recover J_c, but $J_c(\epsilon)$ shows a plateau up to an axial strain where cracks occur and J_c collapses (Fig. 3: *c*). Though $J_c(\epsilon)$ on this plateau is reversible, any additional pre-compression and relaxation causes a wider plateau at a reduced J_c value. Such a wider plateau is often misinterpreted as an indication for reduced strain sensitivity, but is in fact a result of a larger axial pre-compression in the Bi–2212. The J_c loss is on the order of 75% per 1% axial compressive strain [14]. Construction materials that match the thermal contraction of Bi–2212 are therefore preferred. One publication on the stress sensitivity of Bi–2212 cables indicates a broad-face load limit of about 60 MPa [15]. This emphasizes the need for more detailed investigations and accurate stress handling in magnets and/or new conductor reinforcement techniques.

TABLE I

SUMMARY OF TECHNOLOGICAL CHALLENGES IN RELATION TO SUPERCONDUCTOR CHOICE AND ACHIEVABLE DIPOLE MAGNETIC FIELDS.

Material	Dipole limit	Reaction	Wire axial compression	Cable transverse stress	Insulation	Construction	Quench propagation
NbTi	10.5 T	Ductile: R&W	N/A	N/A	Polyimide	Stainless Steel	> 20 ms^{-1}
Nb_3Sn	17–18 T ($F_p \uparrow$: 22 T)	~ 675°C in Ar/Vacuum	Reversible	200 MPa limit	S/R–Glass	Stainless Steel	~ 20 ms^{-1}
Bi–2212	Stress limited	~ 890°C in O_2 ($\pm$ 2°C)	Irreversible	60 MPa limit	Ceramic	Super alloy	~ 0.04 ms^{-1}

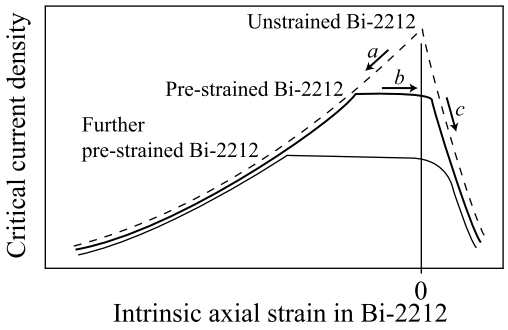

Fig. 3. Model to describe the critical current density as function of axial strain. After ten Haken *et al.* [14].

B. Formation reaction related issues

Bi–2212 is a brittle ceramic material which is formed from precursor powders during a partial melt reaction at about 890°C in an oxygen-rich environment. This higher temperature in comparison with Nb_3Sn, and the presence of oxygen and a partial melt in the wire core, place high demands on the insulation and construction materials in a W&R magnet fabrication process. These problems can in principle be avoided using a React-and-Wind (R&W) process as was demonstrated by other groups [16], [17], at the cost of irrecoverable J_c loss due to strain. To achieve magnetic fields approaching 20 T and higher, a low inductance dipole magnet with small bending radii in the highest field regions is the preferred option. A W&R method is then inevitable to retain high field J_c.

Construction materials will have to withstand the high temperature in an oxygen-rich environment, and match the thermal contraction of Bi–2212 core. Our research indicates that some low-carbon stainless-steel alloys and nickel-based 'Super alloys', such as INCONEL®, would perform adequately.

The choice of insulation materials is limited to ceramics, which have to be chemically compatible with the Bi–2212 formation reaction and available in a form that is suitable for cable insulation. Three problems arise as a result of the partial core-melting and the oxide reaction. First, micro-cracks and pin-holes can be present in the Ag matrix. These can cause liquid core constitutes to leak out and react with the insulation and/or construction materials. Second, oxides in the insulation can etch the Ag matrix materials at the grain boundaries, causing micro-cracks and leakage. Third, insulation components can accelerate the diffusion of core constitutes to the surface of the matrix. It should be emphasized that only limited sources are available that address these issues [18], [19]. ZrO_2, Al_2O_3, Y_2O_3 and high purity SiO_2 are possible candidates, and the presence of Cr, Mg, Ni, and Fe should be avoided. Also, the formation of SiO_2-glass phases should be avoided. The literature, and other sources, are therefore ambiguous regarding pure SiO_2.

TABLE II

SUB-SCALE MAGNET CONFIGURATIONS.

Test layout	Stress on cable [MPa]	Magnetic field [T]
Common coil	0–50	3–5 (Bi–2212 only)
Common coil	0–50	10 (Nb_3Sn + Bi–2212)
Dipole	0–50	3–5 (Bi–2212 only)
Dipole	50–100	12 (Nb_3Sn + Bi–2212)

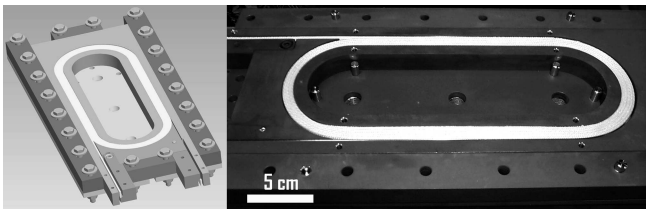

Fig. 4. Bi–2212 sub-scale reaction tooling design (left) and a dummy sub-scale coil inside reaction tooling (right).

IV. BI–2212 TECHNOLOGY DEVELOPMENT AT LBNL

A. Bi–2212 sub-scale magnets

We initiated a program to develop the technology for W&R Bi–2212 magnets. The program goal is to solve the issues discussed in the previous section using sub-scale magnets [20] as a technology test-bed. A number of 2×6 turns double pancake sub-scale coils will be wound from Bi–2212 cable to test insulation and construction materials. Stand alone acceptance tests will be performed on sub-scale coils and successful coils will be stacked into various sub-scale magnet configurations with different magnetic field and load options, as summarized in Table II. A number of coils will be extensively instrumented to study magnet protection issues. Such a modular approach gives the opportunity to efficiently test a variance in materials, loads and magnetic fields. Also, it will enable mechanical decoupling of Nb_3Sn background coils and Bi–2212 coils.

Sub-scale coil heat treatments will initially be performed at Showa Electric Wire and Cable Co., Japan and Oxford Instruments Superconducting Technology, Carteret, NJ (OST), until a suitable furnace becomes available at LBNL. Two dummy sub-scale coils, wound from insulated Ag cables, will be used to study the critical coil heat treatment thermodynamics and to tune the furnaces. Fig. 4 shows the design and a fabricated dummy sub-scale coil inside reaction tooling.

B. Materials development

A combination of oxidation tests at 880°C in pure O_2 and availability yielded INCONEL alloy 600, INCONEL C276, and stainless steel 316L alloys as suitable construction materials for the reaction tooling. INCONEL alloy 600 was selected since this most closely matches the thermal contraction of Bi–2212, whereas bolts, nuts and rings are available in INCONEL C276. All reaction tooling is heat treated in pure oxygen to create an oxide layer before coil winding.

Cable insulation materials can be separated into five groups: 1) Ceramic fiber based sleeve, cloth or tape, 2) Metal-oxides, 3) Ceramic paper, 4) Sol-Gel based ceramic coatings, and 5) Plasma sprayed ceramic coatings. The latter two options were not pursued since at present, the available results on Sol-Gel based coatings on metals and conductors [21], and LBNL's in-house experience on plasma coated metals, do not appear to be sufficiently promising.

Fibers, suitable for braiding, were obtained from 3M™. We have tested, in close collaboration with OST, the following Nextel™ fibers for compatibility with the Bi–2212 formation reaction using short sample tests: 312 ($Al_2O_3/SiO_2/B_2O_3$, 62/24/14%), 440 ($Al_2O_3/SiO_2/B_2O_3$, 70/28/2%), 610 ($Al_2O_3/SiO_2/FeO_3$, >99/<0.3/<0.7%) and 720 (Al_2O_3/SiO_2, 85/15%). We also tested pure SiO_2 (>99.97%) Quartzel® fibers from Saint-Gobain. We found that the fibers containing B_2O_3 are incompatible, but that Nextel 610 and 720, as well as Quartzel fibers are compatible. The compatible Nextel fibers cannot be braided into sleeve of a sufficiently low wall thickness ($< 150\ \mu$m), but are available in cloth. Quartzel fibers were braided into trial sleeve with a wall thickness of about $225\ \mu$m by EDO Fiber Innovations, Walpole, MA. Thinner wall sleeve is presently under development.

Metal-oxide insulation can be used by co-winding a strip of suitable metal that is compatible with the Bi–2212 formation reaction. We tested Ti grade-2, which initially appeared promising, forming a rigid $25\ \mu$m TiO_2 layer and O_2 depleting within a few μm into the Ti base material. Unfortunately, oxide layer growth increased to around $150\ \mu$m when in contact with the Ag-alloy matrix material and sintering occurred. Also, the matrix material became brittle, indicating a reaction between the Ag-alloy and the Ti. Ti is therefore not suitable to form a metal-oxide insulation, but alternatives will be investigated.

The above investigations have highlighted, for now, sleeve from Quartzel fibers as the most suitable insulation option. Coil tests with this insulation will determine large scale applicability and compatibility. Organic sizing, present on the fibers to reduce abrasion, is usually problematic in Nb_3Sn insulations since it can form carbon deposits in the finished coils [22]. Sizing is of less concern for Bi–2212 due to the presence of pure O_2. Some concerns with respect to the compatibility of the sizing constitutes can be raised, but the Quartzel fibers were tested without initial heat cleaning. Their sizing thus does not appear to be problematic, provided it can be completely burned off during a coil reaction.

V. Conclusion

For accelerator dipole magnets NbTi is intrinsically limited to 10.5 T by its field-temperature phase boundary. Nb_3Sn is practically limited to 17 to 18 T due to insufficient high field pinning capacity and, if this could be improved, intrinsically limited to 22 T by its field-temperature phase boundary. To achieve dipole magnetic fields approaching 20 T and higher, a switch to Bi–2212 is inevitable.

A Bi–2212 sub-scale program was initiated in which the required technology for W&R Bi–2212 accelerator magnets will be developed. Insulation and construction materials were investigated and the most suitable options found are, for now, pure SiO_2 braided sleeve insulation and INCONEL construction material. A Bi–2212 sub-scale coil design has been made and a first dummy coil has been fabricated.

Acknowledgment

The authors would like to thank E. E. Hellstrom, K. R. Marken, M. Meinesz and T. Hasegawa for collaborations and helpful discussions, A. Devred for providing a prototype Quartzel braided tape, P. Bish, R. Hannaford, H. C. Higley, D. Horler, N. L. Liggins, G. Ritchie, J. Swanson for their technical expertise and L. Sun for SEM analysis.

References

[1] D. Leroy, *et al.*, in *Proc. of the 15th International Conference on Magnet Technology, Beijing, China*, L. Lianghzhen, S. Guoliao, and Y. Lugang, Eds., vol. 1. Science Press, Beijing, China, 1998, p. 119.
[2] A. F. Lietzke, *et al.*, *IEEE Trans. Appl. Supercond.*, vol. 14, no. 2, p. 345, 2004.
[3] J. A. Parrell, M. B. Field, Y. Zhang, and S. Hong, *Adv. Cryo. Eng. (Materials)*, vol. 50B, p. 369, 2004.
[4] S. A. Gourlay, *et al.*, *IEEE Trans. Appl. Supercond.*, vol. 16, no. 2, p. 324, 2006.
[5] L. Bottura, *IEEE Trans. Appl. Supercond.*, vol. 10, no. 1, p. 1054, 2000.
[6] P. J. Lee and D. C. Larbalestier, *Wire Journal International*, vol. 36, no. 2, p. 61, 2003.
[7] A. Godeke, *Supercond. Sci. and Techn.*, vol. 19, no. 8, p. R68, 2006.
[8] A. Godeke, B. ten Haken, H. H. J. ten Kate, and D. C. Larbalestier, *Supercond. Sci. and Techn.*, vol. 19, p. R100, 2006.
[9] A. Godeke, *et al.*, *J. Appl. Phys.*, vol. 97, p. 093909, 2005.
[10] D. Uglietti, *et al.*, "Composition, grain morphology and transport properties of Nb_3Sn Bronze Route and Internal Sn wires," Presentation THA01PO06 at the 19th International Conference on Magnet Technology, Genova, Italy, 2005.
[11] L. D. Cooley, P. J. Lee, and D. C. Larbalestier, *Adv. Cryo. Eng. (Materials)*, vol. 48B, p. 925, 2002.
[12] U. P. Trociewitz, *et al.*, *NHMFL Reports 2006*, vol. 13, no. 1, p. 31, 2006.
[13] K. Marken, *et al.*, "Progress in Bi–2212 wire and coils for superconducting magnets," Presentation HH4.6 at the MRS Spring Meeting, San Francisco, CA, USA, April 19, 2006.
[14] B. ten Haken, A. Godeke, H. J. Schuver, and H. H. J. ten Kate, *IEEE Trans. Magn.*, vol. 32, no. 4, p. 2720, 1996.
[15] D. R. Dietderich, *et al.*, *IEEE Trans. Appl. Supercond.*, vol. 11, no. 1, p. 3577, 2001.
[16] R. Gupta, *et al.*, *IEEE Trans. Appl. Supercond.*, vol. 14, no. 2, p. 1198, 2004.
[17] H. W. Weijers, *et al.*, *Supercond. Sci. and Techn.*, vol. 17, p. 634, 2004.
[18] D. E. Wesolowski, *et al.*, *Supercond. Sci. and Techn.*, vol. 18, p. 934, 2005.
[19] I. H. Mutlu, E. Celik, and Y. S. Hascicek, *Physica C*, vol. 370, p. 113, 2002.
[20] R. R. Hafalia, *et al.*, *IEEE Trans. Appl. Supercond.*, vol. 13, no. 2, p. 1258, 2003.
[21] F. Buta, *et al.*, *Adv. Cryo. Eng. (Materials)*, vol. 50A, p. 273, 2003.
[22] A. Devred, *IEEE Trans. Appl. Supercond.*, vol. 12, no. 1, p. 1232, 2002.